AIAA'88

AIAA-88-3611-CP

On Mixing and Structure of the Concentration Field of Turbulent Jets

David R. Dowling and Paul E. Dimotakis, California Institute of Technology, Pasadena, CA

AIAA/ASME/SIAM/APS 1st Fluid Dynamics Congress

July 25-28, 1988/Cincinnati, Ohio

For permission to copy or republish, contact the Amerian Institute of Aeronautics and Astronautics
370 L'Enfant Promemade, S.W., Washington, D.C. 20024

ON MIXING AND STRUCTURE OF THE CONCENTRATION FIELD OF TURBULENT JETS

88-3611-CP

David R. Dowling† and Paul E. Dimotakis*

Graduate Aeronautical Laboratories
California Institute of Technology
Pasadena, California 91125

Abstract

This work is an investigation of the mixing of the nozzle fluid of a round turbulent jet with the entrained reservoir fluid, using laser-Rayleigh scattering methods. Our measurements, at a Reynolds number of 5000, cover the axial range from 20 to 80 jet exit diameters and resolve the full range of temporal & spatial concentration scales. The measured mean & rms values of the concentration, and the mean scalar dissipation rate, when estimated from the time derivative of concentration, are consistent with jet similarity laws. Concentration fluctuation power spectra are found to be self-similar along rays emanating from the jet virtual origin. The probability density functions for the concentration, the time derivative of concentration, and the square of the time derivative of concentration, are compiled and are also self-similar along rays.

Introduction

Background

The free turbulent jet, a small source of high speed fluid issuing into a large quiescent reservoir, is one of the classical free shear flows. It has been the subject of experimental work for more than 50 years (Ruden[23] 1933, Kuethe[15] 1935) and has found broad application in combustion systems as a means of mixing reactants.

It is conventionally accepted that profiles of the mean jet fluid concentration are self-similar beyond about 20 jet exit diameters (Wilson & Dankwerts[27] 1964, Becker et al.[3] 1967, Birch et al.[4] 1978, Lockwood & Moneib[16] 1980). In cylindrical coordinates with the direction of the jet discharge chosen to lie along the axis of symmetry (the x-axis here), the mean profile of jet gas concentration, for example, takes the following form:

$$\overline{C}(x,r) = \frac{C_0}{x - x_0} F\left(\frac{r}{x - x_0}\right) \qquad (1)$$

where r is the radial coordinate, C_0 the jet gas concentration at the nozzle exit, F is a smooth function that is experimentally determined, x_0 is the virtual origin, and the overbar denotes a time average.

---

† Presently, Senior Specialist Engineer, Boeing Aerospace, P.O. Box 3999 M/S 8H-29 Seattle, Washington 98124

* Professor, Aeronautics & Applied Physics, Member AIAA

Copyright © 1988 by David R. Dowling. Published by the American Institute of Aeronautics and Astronautics Inc. with permission.

While the similarity of the mean profile is on a solid experimental footing, the picture is not yet complete. Most experimental data for the root mean square (rms) fluctuation can not be collapsed in the same coordinates used to collapse the mean values. Conflicts also exist between the reported rms levels from different experiments (Dahm[8] 1985). No clear consensus exists as to whether the ratio of the rms to mean concentration of the jet fluid ($C'_{rms}/\overline{C}$) is a constant in the far field of the jet (Dahm[8] 1985). These problems could arise from many sources including: Reynolds number effects, contamination of the flow by small buoyancy forces, insufficient resolution of all of the fluctuating scales, unsteadiness in the jet source or the quiescent reservoir, neglect of the effects of the molecular Schmidt number (kinematic viscosity divided by species diffusivity), or the possible failure of the chosen similarity form.

Present Experiments

The experiments described here address some of these concerns in the far-field of the jet. These experiments were designed with adequate spatial & temporal resolution, as well as dynamic range, throughout the jet to unambiguously resolve all of the diffusion scales in a purely momentum dominated flow. This meant that the Reynolds number, nozzle size, jet & reservoir gases and internal volume of the experimental enclosure were not chosen independently of each other or of the noise characteristics of the diagnostic.

This work, an experimental investigation of mixing of the jet fluid with the entrained reservoir fluid, is based on measurements of the instantaneous concentration of jet fluid, $C(t)$. In particular, it is a study of the similarity of the mean concentration of jet fluid, $\overline{C}$, the probability density function of jet fluid concentration, the rms fluctuation level, C'_{rms}, the power spectrum of concentration fluctuations, E_C, the probability density function of the time derivative of concentration, and some of the statistical properties of the scalar dissipation rate, ε_C, as estimated from the square of the time derivative of concentration.

Experimental Technique

The Main Apparatus

These experiments were performed in the gas phase jet mixing apparatus shown schematically in Figure 1. The main apparatus consisted of a large enclosure with an interior volume of about 120 cubic feet. The jet was produced by a vertically adjustable $\frac{3}{4}$" nozzle with an 11 to 1 contraction ratio. The exit turbulence level was less than 0.2% and the exit Reynolds number ($U_0 d/\nu_\infty$) was 5000, where ν_∞ is the reservoir gas kinematic viscosity. The Taylor Reynolds number along the

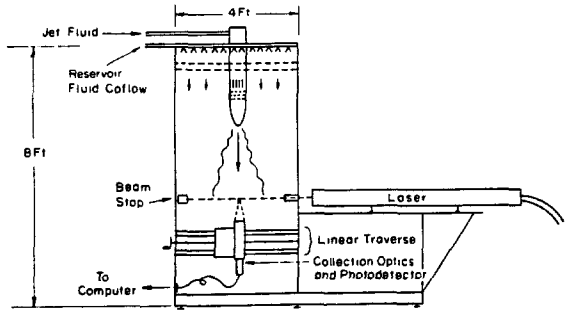

Figure 1. Experimental facility.

centerline of the jet was estimated from the formulae in Hinze[13] (1975), Equations 5 & 6 (see page 4), and a typical value for the centerline rms velocity fluctuation, $u'_{rms} \approx .25\,\bar{U}_{cl}$. The result being: $Re_\lambda \approx 100$. A uniform coflow velocity, typically about 0.006 of the jet velocity, was produced over the entire 16 ft^2 cross section of the enclosure. The volume flux of the coflow was chosen to provide the entrainment needs of the jet (Ricou & Spalding[22] 1961) to a point down below the farthest measuring station. Large 3' x 5' plexiglas windows were located on opposite sides of the enclosure to allow shadowgraph imaging of the jet. The exhaust gases from the experiment exited through the bottom of the enclosure and were collected in a large plastic bag.

The jet gas was ethylene, C_2H_4, and its flow rate was set with a single stage regulator and a metering valve. The dynamic head of the jet was measured to determine U_o. The reservoir and coflow gas was N_2. The coflow was produced by regulating the pressure of a special delivery manifold. The density ratio of ethylene to N_2 is 1.0015. An axisymmetric laminar boundary layer calculation was used to estimate boundary layer thicknesses at the nozzle exit to calculate the the momentum diameter of the nozzle, d^*, introduced in a limited way by Thring & Newby[24] (1952), used by Avery & Faeth[1] (1974), and modified by Dahm & Dimotakis[7] (1987) to:

$$d^* = \frac{2\dot{m}_o}{\sqrt{\pi \rho_\infty J_o}} \qquad (2)$$

where $\dot{m}_o$ & J_o are the nozzle mass and momentum fluxes respectively, and the density of the reservoir fluid is denoted by ρ_∞. The estimate for the nozzle conditions of these experiments was $d^* = 0.96d$. Note that the momentum diameter, d^*, reduces to the geometric exit diameter, d, for $\rho_{jet} = \rho_\infty$ and a perfect "top-hat" exit profile of velocity.

The Diagnostic

Laser-Rayleigh scattering was used to determine the concentration time history of the binary mixture of jet and reservoir gases within a small focal volume in the mixing region of the jet. This non-intrusive diagnostic has been successfully used by many previous authors (Dyer[10] 1979, Escoda & Long[11] 1983, Pitts & Kashiwagi[19] 1984, Pitts[20] 1986, and others) and will not be described here. The main difference between this work and previous implementations of this technique was the strict observance of the spatial and temporal resolution requirements imposed by the need to accurately record the smallest estimated diffusion scales of the flow.

For these experiments, the Rayleigh scattered light from a short section of an 18 Watt collimated laser beam was imaged (one to one) onto a small aperture photodiode. The diameter of the sensitive area of the photodiode was between .20 and 1.0 mm; the local resolution requirements of the jet dictating the size used in each case. The signal current from the photodiode was amplified by a low-noise transimpedance amplifier designed by Dr. Dan Lang. This signal was filtered and sent to an LSI PDP-11/73 based computer system where it was digitized and stored for subsequent processing. The sampling frequency and filter bandwidth were chosen to insure that the estimated temporal resolution requirements imposed by the jet were surpassed by more than a factor of four. The sensitivity of the whole system was calibrated by introducing pure jet and reservoir gases into the focal volume before and after each run.

Results

The Mean and RMS Profiles

The properly scaled mean and rms concentration profiles for x/d = 20, 40, 60, & 80 are shown on Figure 2. The transformation used to collapse both profiles is based only on the experimentally fitted values of the virtual

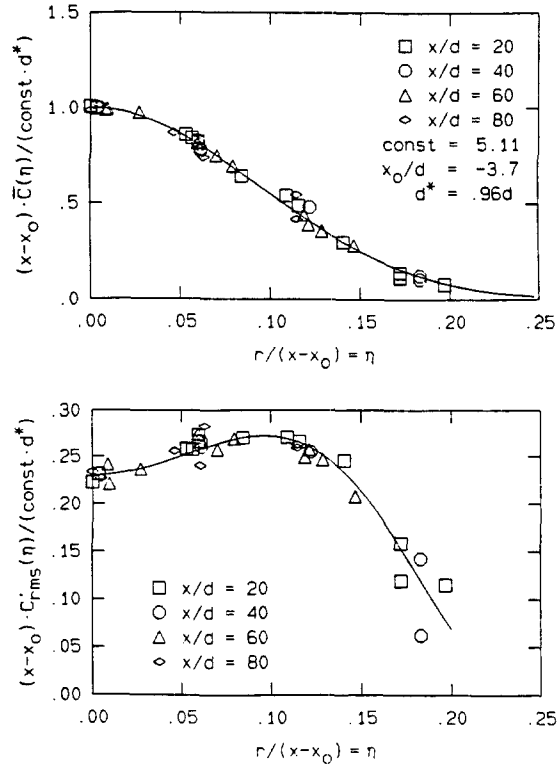

Figure 2. Mean and rms profiles of concentration.

origin, x_o, and the decay constant for the mean centerline concentration. Separate normalizations by the local centerline mean, centerline rms concentration, or concentration profile half radius were not necessary.

Probability Density Function of Concentration

The probability density function for the jet gas concentration was estimated by sorting the sampled data into a histogram. The results are plotted in Figures 3, 4, & 5 and display the

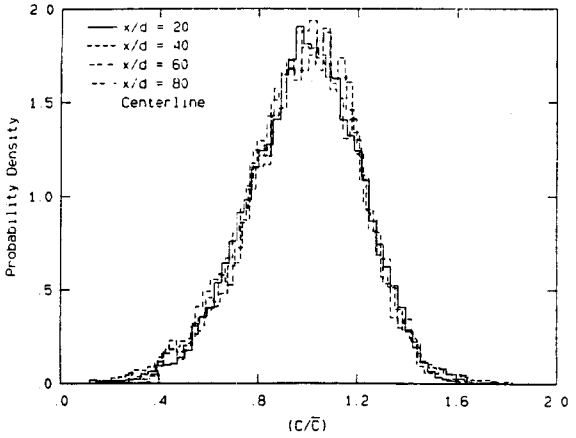

Figure 3. Probability density function of the scaled concentration on the centerline of the jet.

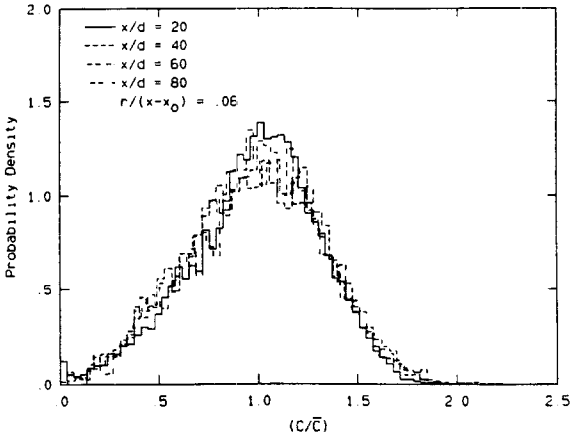

Figure 4. Probability density function of the scaled concentration 3.5° off the centerline of the jet.

similarity collapse of the concentration PDF along the centerline ray ($r/(x-x_o) = 0$), along a ray at 3.5° ($r/(x-x_o) \approx .06$), and along a ray at 7° ($r/(x-x_o) \approx .12$). The visual edge of the jet is at about 12° (White[25] 1974). Imperfections in the collapse, which are more evident as the edge of the jet is approached, are believed to be caused

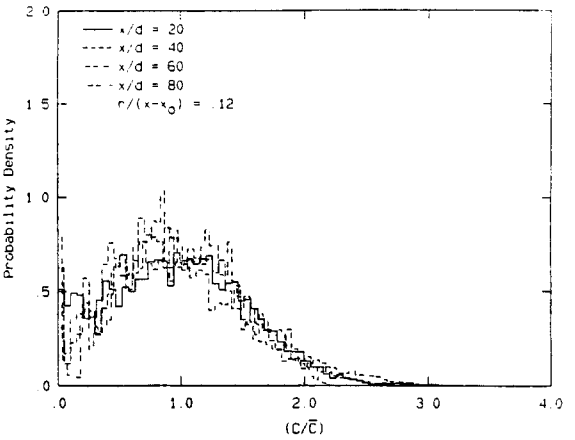

Figure 5. Probability density function of the scaled concentration 7° off the centerline of the jet.

by decreased statistical convergence. In particular, for a fixed run time, the total volume of fluid that passes through the focal volume is roughly proportional to the local mean velocity. Consequently, the effective sample size of a run is smaller near the edge of the jet.

Power Spectrum of Concentration Fluctuations

The power spectra of the concentration fluctuations were calculated from the sampled data sets for x/d = 20, 40, 60, & 80 along the three rays at $r/(x-x_o) \approx 0$, .06, & .12. The results are plotted in Figures 6, 7, & 8 where τ_ℓ

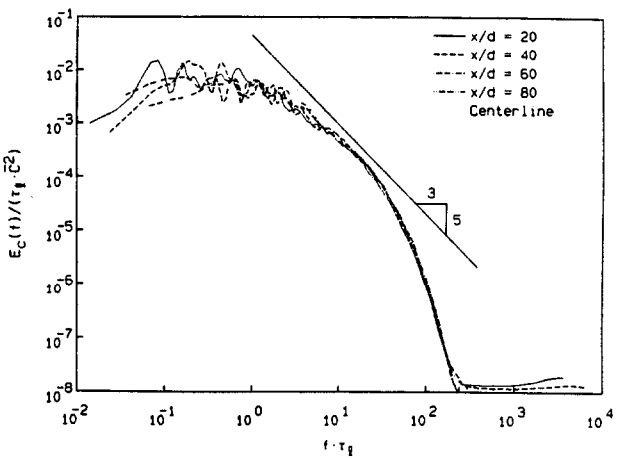

Figure 6. Scaled power spectra of the concentration fluctuations on the centerline of the jet.

(= local jet diameter/local mean centerline velocity) is the estimated large-scale time of the jet. The computed spectra satisfy the relation

$$\left[2 \int_0^\infty E_c(f)\, df \right]^{1/2} = C'_{rms} \qquad (3)$$

as an overall normalization. The flat portion of

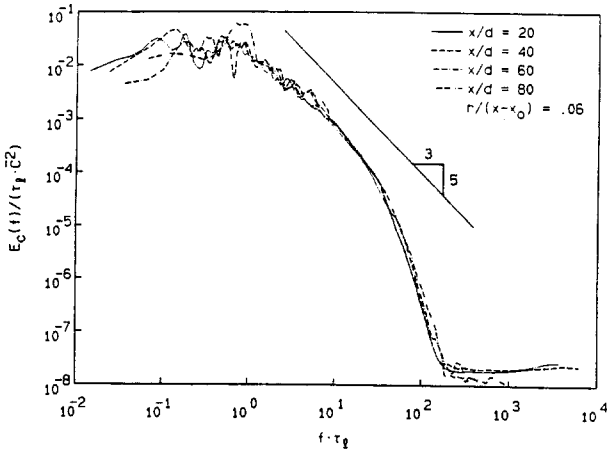

Figure 7. Scaled power spectra of the concentration fluctuations 3.5° off the centerline of the jet.

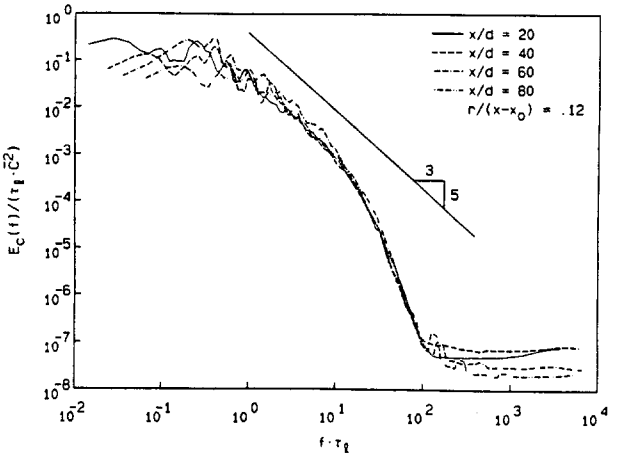

Figure 8. Scaled power spectra of the concentration fluctuations 7° off the centerline of the jet.

each spectrum at high frequencies is the noise floor produced by the measurement technique.

The spectra collapse fairly well in spite of the modest Reynolds number of the jet flow. The calculated value of the Kolmogorov passage frequency, f_K, should roughly correspond to the high frequency end of the - 5/3 slope when the molecular Schmidt is of order one (Batchelor[2] 1959, Monin & Yaglom[17] 1975). To estimate f_K, the foundation of the temporal resolution requirement, the centerline energy dissipation rate in the jet, $\bar{\varepsilon}$, reported by Friehe et al.[12] (1971), and the mean centerline velocity decay law suggested by Chen & Rodi[5] (1979) were used, i.e.

$$f_K = \bar{U}_{cl} \left(\frac{\bar{\varepsilon}}{\nu_\infty^3} \right)^{1/4} \qquad (4)$$

where:

$$\bar{\varepsilon} = 48. \frac{U_o^3}{d} \left(\frac{x - x_o}{d} \right)^{-4}, \qquad (5)$$

$$\bar{U}_{cl} = 6.2\, U_o \left(\frac{x - x_o}{d} \right)^{-1}. \qquad (6)$$

These formulae and the parameters of the experiments lead to an estimate for $f_K \cdot \tau_\ell$ of about 700. While the spectra reported here do not display a - 5/3 slope, the scaled frequency range in which they begin to fall more rapidly than a constant power law is at least an order of magnitude lower than 700. This discrepancy between the measured and calculated break points has also been reported by Clay[6] (1973) who worked with data from a heated air jet at a Reynolds number of almost 10^6.

It is also worth noting that although the spectra collapse along rays, the spectra are different from ray to ray. In particular, the spectra along the ray at 7° show a longer power law region with a slope closer to - 5/3 than those from the inner rays. This latter behavior was also reported by Lockwood & Moneib[16] (1980) for their measurements at x/d = 20 in a heated air jet at a Reynolds number of 50,000.

The Time Derivative of Concentration

The power spectrum of each data set was used to estimate the optimal (Wiener[26] 1949) filter for that data set (see also Press et al.[21] 1986). The resulting optimal filter was used in each case to eliminate virtually all of the noise from the data, permitting a time derivative to be computed fairly reliably.

The probability density functions of the scaled time derivative were compiled. The results are displayed in Figures 9, 10, & 11. The self-similarity of the data aside, several other

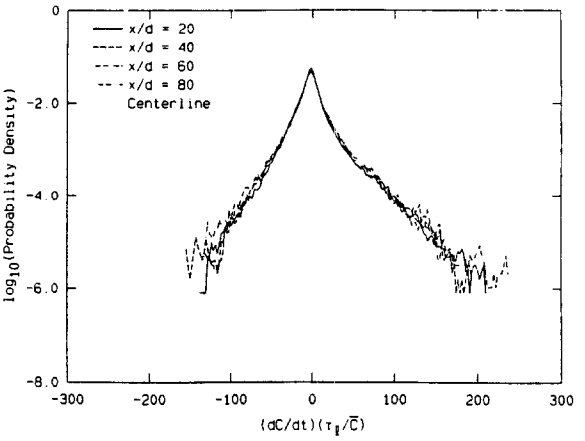

Figure 9. Probability density function of the scaled concentration time derivative on the jet centerline.

interesting points are noteworthy. All three curves are asymmetrical with the peaks slightly off center. One explanation for this is evident in the time traces of the data, which show many more large positive slopes than negative ones. In

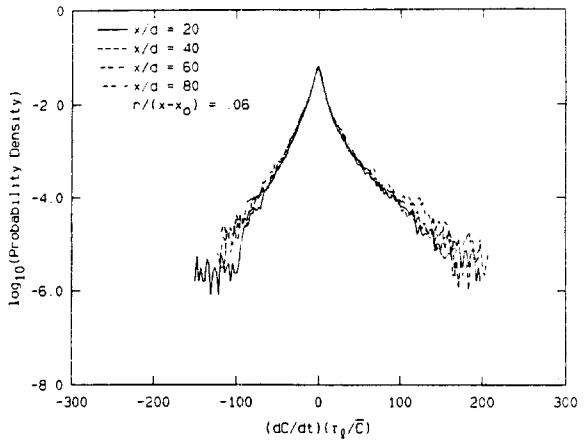

Figure 10. Probability density function of the scaled concentration time derivative 3.5° off the jet centerline.

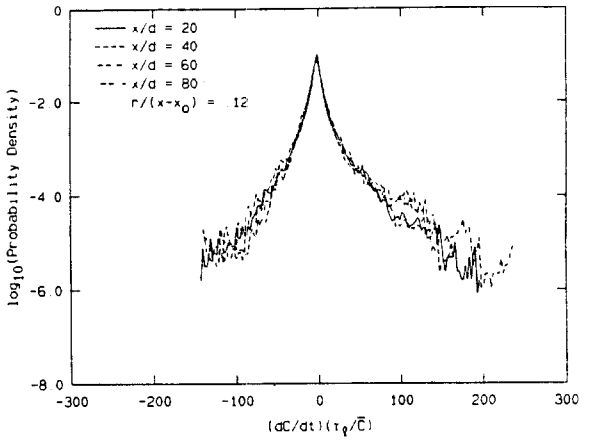

Figure 11. Probability density function of the scaled concentration time derivative 7° off the jet centerline.

fact there seems to be a "typical" large scale structure associated with the flow that takes the form of a sharp rise followed by a region where the concentration falls choatically, at a lower average rate, until the next sharp rise. Some typical data traces showing this behavior are depicted on Figure 12. The large scale time corresponding to the plotted data is estimated to be about 1.3 seconds, or about half each line's time span.

The Estimated Scalar Dissipation Rate

The scalar dissipation rate is the instantaneous rate of local mixing of the jet and reservoir gases. By squaring and scaling the concentration time derivative an estimate of the scalar dissipation rate, ε_c, can be made. Here we have used only the mean centerline velocity to

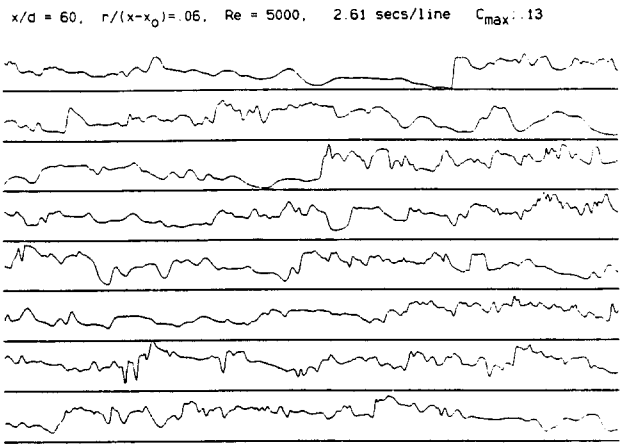

Figure 12. Time traces of the instantaneous jet gas concentration.

scale the time derivative:

$$\varepsilon_c = 3 D_{j\infty} \left(\frac{1}{\bar{U}_{cl}} \frac{dC}{dt} \right)^2 \qquad (7)$$

where $D_{j\infty}$ is the diffusivity of jet gas into reservoir gas. A plot of the mean estimated scalar dissipation rate, computed from the data along the three rays at $r/(x-x_o)$ = .0, .06, & .12, is shown on Figure 13. The scaling of the

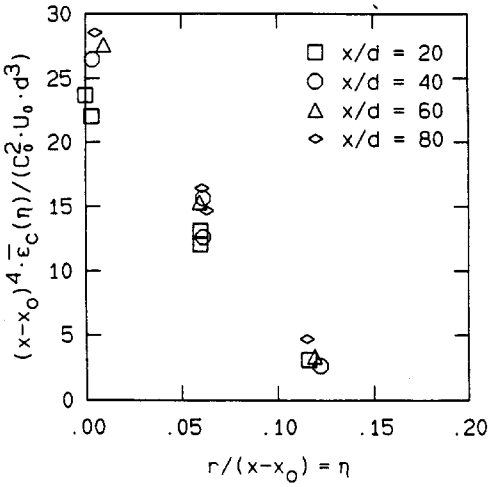

Figure 13. Scaled mean value of the scalar dissipation rate when estimated from $(dC/dt)^2$.

vertical axis is consistent with that suggested by Friehe et al.[12] (1971) for the energy dissipation rate. We note that even though this plot is severely leveraged by a factor of $(x-x_o)^4$, the collapse is acceptable, especially since the data at x/d = 20 may be contaminated by near-field effects.

Classical theories of turbulence at high Reynolds number (Kolmogorov[14] 1962, Obukhov[18] 1962) predict that the probability density function of $(dC/dt)^2$ should be log-normal. The current data are at a modest Reynolds number so they can, at most, provide a test to determine the lower Reynolds number limit of some of the classical ideas. A log-normal distribution is Gaussian when plotted verses a logarithmic abscissa and a linear ordinate. The scaled results of these experiments for $(dC/dt)^2$ are plotted in such log-linear coordinates on Figures 14, 15, and 16 for x/d = 20, 40, 60, & 80 along

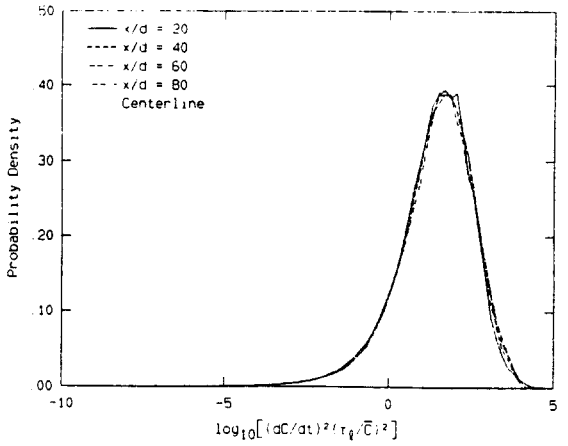

Figure 14. Probability density function of the logarithm of $(dC/dt)^2$ on the jet centerline.

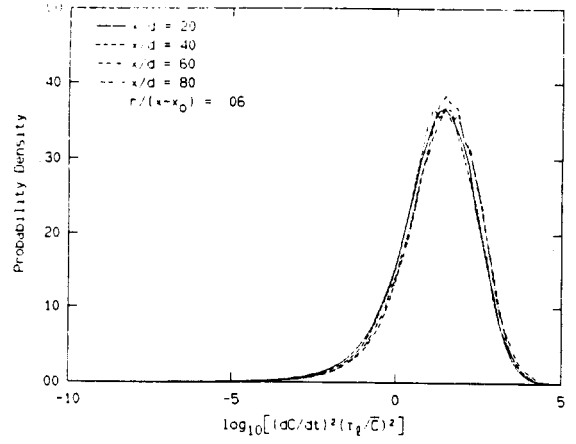

Figure 15. Probability density function of the logarithm of $(dC/dt)^2$ 3.5° off the jet centerline.

the three rays at $r/(x-x_o) \approx 0$, .06, & .12. The compiled curves look approximately Gaussian but all display a relative excess at low values and a relative deficit at high values. It is also worth noting that the full width at half maximum of the distributions is typically 3 or more orders of magnitude. To the extent that $(dC/dt)^2$ scales the

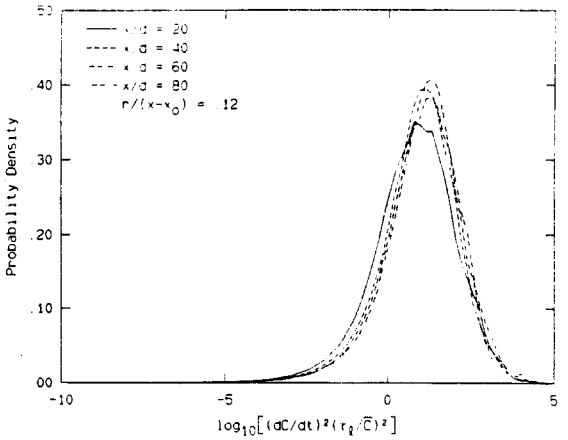

Figure 16. Probability density function of the logarithm of $(dC/dt)^2$ 7° off the jet centerline.

local mixing rate, this result has important implications for the description and modeling of turbulent mixing, with or without chemical reactions and combustion.

Conclusions

Figures 2 through 16 make a compelling case for complete similarity of the mixing at all scales in the far-field of a momentum driven jet. These plots establish that the local mean concentration and the local large-scale time can be used to collapse the statistical measures of the fluctuating concentration field of the jet at a Reynolds number of 5000. Our most recent experiments (see Dowling[9] 1988) suggest that this self-similarity extends to higher Reynolds numbers. Additionally, the measurements presented in this paper show that some of the classical theories of turbulence can be applied at Reynolds numbers which might not be considered high enough for the flow to have reached a Reynolds number independent state.

Acknowledgements

The authors wish to acknowledge Dr. Daniel B. Lang for his assistance in the design and fabrication of the whole data acquisition system. This work was supported by the Gas Research Institute grant # 5083-260-0878 and the Air Force Office of Scientific Research contract # 83-0213.

References

1. AVERY, J.F. and FAETH, G.M. 1974, "Combustion of a submerged gaseous oxidizer jet in liquid metal," Fifteenth (International) Symposium on Combustion, The Combustion Institute.

2. BATCHELOR, G.K. 1959, "Small-scale variation of convected quantities like temperature in turbulent fluid," J. Fluid Mech., 5, 113.

3. BECKER, H.A., HOTTEL, H.C. and WILLIAMS G.C. 1967, "The nozzle fluid concentration field of the round turbulent jet," J. Fluid Mech., 30, 285-303.

4. BIRCH, A.D., BROWN, D.R., DODSON, M.D., and THOMAS, J.R. 1978, "The turbulent concentration field of a methane jet," J. Fluid Mech., 88, 431-449.

5. CHEN, C.J. and RODI, W. 1980, Vertical Turbulent Buoyant Jets: A Review of Experimental Data, (Pergamon Press, New York).

6. CLAY, J.P. 1973, "Turbulent mixing of temperature in air, water and mercury," Ph.D. Thesis, University of California San Diego.

7. DAHM, W.A. and DIMOTAKIS, P.E. 1987, "Measurements of entrainment and mixing in Turbulent jets," AIAA J. 25(9), 1216-1223.

8. DAHM, W.A. 1985, "Experiments on entrainment, mixing and chemical reactions in turbulent jets at high Schmidt number," Ph.D. Thesis, Caltech.

9. DOWLING, D.R. 1988, "Mixing in gas phase turbulent jets," Ph.D. Thesis, Caltech.

10. DYER, T.M. 1979, "Rayleigh scattering measurements of time-resolved concentration in a turbulent propane jet," AIAA Journal, 17, 912.

11. ESCODA, M.C. and LONG, M.B. 1983, "Rayleigh scattering measurements of the gas concentration field in turbulent jets," AIAA Journal, 21, 81.

12. FRIEHE, C.A., VAN ATTA, C.W., and GIBSON, C.H. 1971, "Jet turbulence: dissipation rate measurements and correlations," AGARD Turbulent Shear Flows, CP-93, 18-1 to 18-7.

13. HINZE, J.O. 1975, Turbulence, 2nd ed. (McGraw-Hill Book Co., New York), p. 224-225.

14. KOLMOGOROV, A.N. 1962, "A refinement of the previous hypotheses concerning the local structure of turbulence in a viscous incompressible fluid at high Reynolds number", J. Fluid Mech. 13, 82-85.

15. KUETHE, A.M. 1935, "Investigations of the turbulent mixing regions formed by jets," Journal of Applied Mechanics, Transactions of the AMSE, Vol. 2, no. 3, 87-95.

16. LOCKWOOD, F.C. and MONIEB, H.A. 1980, "Fluctuating temperature measurements in a heated round free jet," Comb. Sci. Tech., 22, 63-81.

17. MONIN, A.S., and YAGLOM A.M. 1975, Statistical Fluid Mechanics II, (MIT Press, Cambridge), Chapter 8.

18. OBUKHOV, A.M. 1962, "Some specific features of atmospheric turbulence", J. Fluid Mech. 13, 77-81.

19. PITTS, W.M., and KASHIWAGI T. 1984, "The application of laser-induced Rayleigh light scattering to the study of turbulent mixing," J. Fluid Mech. 141, 391.

20. PITTS, W.M. 1986, "Effects of global density and Reynolds number variations on mixing in turbulent axisymmetric jets," NBSIR 86-3340.

21. PRESS, W.H., FLANNERY, B.P., TEUKOLSKY, S.A., and VETTERLING, W.T. 1986, Numerical Recipes (Cambridge University Press, New York), p. 417-419.

22. RICOU, F.P., and SPALDING, D.B. 1961, "Measurements of entrainment by axisymmetrical turbulent jets," J. Fluid Mech. 11, 21.

23. RUDEN, P. 1933, "Turbulente aurbreitungsvorgänge im freistrahl," Die Naturwissenshaften, Jahrg. 21, Heft. 21/23, 375-378.

24. THRING, M.W. and NEWBY, M.P. 1952, "Combustion length of enclosed turbulent jet flames", Fourth (International) Symposium on Combustion, The Williams and Wilkins Co., 789.

25. WHITE, F.M. 1974, Viscous Fluid Flow, (McGraw-Hill Book Company, New York), p. 505-510.

26. WIENER, N. 1949, Extrapolation, Interpolation and Smoothing of Stationary Time Series, (Technology Press, MIT & John Wiley).

27. WILSON, R.A.M. and DANKWERTS, P.V. 1964, "Studies in turbulent mixing - II, A hot air jet," Chem. Engr. Sci. 19, 885-895.